

---

# Reinforcement Learning via Conservative Agent for Environments with Random Delays

---

**Jongsoo Lee\***  
jjongs@postech.ac.kr

**Jangwon Kim\***  
jangwonkim@postech.ac.kr

**Jiseok Jeong\***  
wlw19865@postech.ac.kr

**Soohee Han\***  
soohee.han@postech.ac.kr

## Abstract

Real-world reinforcement learning applications are often hindered by delayed feedback from environments, which violates the Markov assumption and introduces significant challenges. Although numerous delay-compensating methods have been proposed for environments with constant delays, environments with random delays remain largely unexplored due to their inherent variability and unpredictability. In this study, we propose a simple yet robust agent for decision-making under random delays, termed the *conservative agent*, which reformulates the random-delay environment into its constant-delay equivalent. This transformation enables any state-of-the-art constant-delay method to be directly extended to the random-delay environments without modifying the algorithmic structure or sacrificing performance. We evaluate the conservative agent-based algorithm on continuous control tasks, and empirical results demonstrate that it significantly outperforms existing baseline algorithms in terms of asymptotic performance and sample efficiency.

## 1 Introduction

Reinforcement learning (RL) has achieved remarkable progress across various domains, from gaming (Mnih et al., 2013; Silver et al., 2016) to robotic control systems (Haarnoja et al., 2018; Kalashnikov et al., 2018). However, real-world RL applications often encounter challenges due to delays, such as network latency in communication systems and response lags in robotic control systems (Ge et al., 2013; Abadía et al., 2021). These delays can significantly degrade the performance of RL agents and even destabilize dynamic systems (Hwangbo et al., 2017; Mahmood et al., 2018).

Although numerous delay-compensating methods have been proposed within the RL framework, most rely on the unrealistic assumption of constant delays (Chen et al., 2021; Derman et al., 2021; Liotet et al., 2022; Kim et al., 2023; Wu et al., 2024b,a), leaving random delays relatively unexplored due to their inherent variability and unpredictability. The stochastic nature of random delays complicates the direct adaptation of conventional constant-delay methods that depend on structured historical information, making it difficult to select appropriate reference points in the past and to identify causal relationships between observations distorted by such delays.

In this study, we propose a *conservative agent* for robust decision-making under random delays. This agent transforms the random-delay environment into its constant-delay equivalent, providing a straightforward plug-in framework that enables the direct application of any constant-delay method to random-delay environments without requiring modifications to the algorithmic structure or incurring performance degradation. We instantiate the conservative agent within the belief projection-based

---

\*Computational, Control Engineering Lab., Pohang University of Science and Technology (POSTECH).

Q-learning (BPQL) framework (Kim et al., 2023), yielding the conservative-BPQL algorithm. Evaluations on continuous control tasks from the MuJoCo benchmark (Todorov et al., 2012) demonstrate that conservative-BPQL consistently outperforms existing baseline algorithms in terms of both asymptotic performance and sample efficiency under random delays.

## 2 Backgrounds

### 2.1 Delay-free Reinforcement Learning

A Markov decision process (MDP) (Bellman, 1957) is defined with a five-tuple  $(\mathcal{S}, \mathcal{A}, \mathcal{P}, \mathcal{R}, \gamma)$ , where  $\mathcal{S}$  and  $\mathcal{A}$  represent the state and action spaces,  $\mathcal{P} : \mathcal{S} \times \mathcal{A} \times \mathcal{S} \rightarrow [0, 1]$  is the transition kernel,  $\mathcal{R} : \mathcal{S} \times \mathcal{A} \rightarrow \mathbb{R}$  is the reward function, and  $\gamma \in (0, 1)$  is a discount factor. Additionally, a policy  $\pi : \mathcal{S} \times \mathcal{A} \rightarrow [0, 1]$  maps the state-to-action distribution.

At each discrete time step  $t$ , an agent observes a state  $s_t \in \mathcal{S}$  from the environment, selects an action  $a_t \in \mathcal{A}$  according to  $\pi$ , receives a reward  $r_t = \mathcal{R}(s_t, a_t)$ , and then observes the next state  $s_{t+1}$ . The agent repeats this process to find an optimal policy  $\pi^*$  that maximizes the expected discounted cumulative reward (i.e., return) over a finite or infinite-horizon  $H$ , which is given as:

$$\pi^* = \operatorname{argmax}_{\pi} \mathbb{E} \left[ \sum_{k=0}^{H-1} \gamma^k r_{k+1} \mid \pi, d_0 \right], \quad (1)$$

where  $d_0$  denotes the initial state distribution. The value functions are defined as:

$$V^\pi(s) = \mathbb{E} \left[ \sum_{k=0}^{H-1} \gamma^k r_{t+k+1} \mid s_t = s, \pi \right], \quad Q^\pi(s, a) = \mathbb{E} \left[ \sum_{k=0}^{H-1} \gamma^k r_{t+k+1} \mid s_t = s, a_t = a, \pi \right], \quad (2)$$

where  $V^\pi(s)$  denotes the expected return starting from state  $s$  under the policy  $\pi$ , and  $Q^\pi(s, a)$  represents the expected return starting from state  $s$ , taking action  $a$ , and thereafter following  $\pi$ .

Note that the dynamics governing MDPs assume the Markov property, implying that the complete probability distribution in the dynamics can be fully determined by the present state and action, independent of their histories. However, delayed environmental feedback can violate this fundamental assumption, significantly degrading the performance of RL agents and even causing complete failure in learning (Singh et al., 1994).

### 2.2 Delayed Reinforcement Learning

In environments with delays, termed delayed MDPs, the state may not be observed by the agent immediately (observation delay,  $\Delta T_s$ ), a lag may exist in determining an action (inference delay,  $\Delta T_i$ ), and the effect of the action may also be delayed (execution delay,  $\Delta T_e$ ). These delays force the agent to make decisions based on outdated information and prevent timely actions, disrupting the overall learning process. Fortunately, only the total delay  $\Delta T = \Delta T_s + \Delta T_i + \Delta T_e$  matters for decision-making (Wang et al., 2023), allowing different types of delays to be treated equivalently. This simplifies the analysis by allowing us to focus on a single type of delay. Based on this rationale, we concentrate on the case of observation delays without loss of generality.

In particular, random observation delays can cause states to be observed out of chronological order, with multiple states being observed simultaneously or the order being completely scrambled. To avoid ambiguity in the decision-making process, we explicitly distinguish between the events of state generation, observation, and usage, as defined below. In this study, we investigate environments with random observation delays under an ordering assumption, where any observed state can be used for decision-making only after all previously generated states have been both observed and used.

**Definition 2.1.** A state is considered *generated* when the environment responds to an agent’s action, *observed* when the resulting state information reaches the agent, and *used* when the agent utilizes it to make a decision by feeding it into the policy.

## 3 Complete Information Method

The complete information method, also known as the augmentation-based approach, is often preferred in environments with delays, as it can restore the Markov property disrupted by delays and enables

policy learning using conventional RL algorithms. This approach involves state reconstruction, where the most recently observed state is combined with the sequence of historical actions to form an augmented state. As demonstrated by Altman and Nain (1992); Katsikopoulos and Engelbrecht (2003), any delayed MDP can be transformed into an equivalent delay-free MDP via state augmentation, and the optimal policies in the transformed MDPs remain optimal in the original delayed MDPs. In this section, we investigate two types of delayed MDPs: the constant-delay MDP (CDMDP) and the random-delay MDP (RDMDP).

### 3.1 Constant-Delay MDP

A CDMDP is defined as a six-tuple  $(\mathcal{S}, \mathcal{A}, \mathcal{P}, \mathcal{R}, \gamma, \Delta)$ , where  $\Delta \in \mathbb{Z}_{>0}$  denotes a constant observation delay. This can be transformed into an equivalent delay-free MDP  $(\mathcal{X}, \mathcal{A}, \mathcal{P}_\Delta, \mathcal{R}_\Delta, \gamma)$ , where  $\mathcal{X} = \mathcal{S} \times \mathcal{A}^\Delta$  is the augmented state space with  $\mathcal{A}^\Delta$  being the Cartesian product of  $\mathcal{A}$  with itself for  $\Delta$  times,  $\mathcal{P}_\Delta : \mathcal{X} \times \mathcal{A} \times \mathcal{X} \rightarrow [0, 1]$  is the augmented transition kernel and  $\mathcal{R}_\Delta : \mathcal{X} \times \mathcal{A} \rightarrow \mathbb{R}$  is the augmented reward function. Additionally, the augmented state-based policy  $\pi_\Delta : \mathcal{X} \times \mathcal{A} \rightarrow [0, 1]$  maps the augmented state-to-action distribution.

Specifically, the augmented state  $x \in \mathcal{X}$  at time  $t$  is defined as:

$$x_t = (s_{t-\Delta}, a_{t-\Delta}, a_{t-\Delta+1}, \dots, a_{t-1}), \quad \forall t > \Delta, \quad (3)$$

where  $s_{t-\Delta}$  is the most recently observed state and  $(a_i)_{i=t-\Delta}^{t-1}$  is the sequence of historical actions. The augmented transition kernel is then defined as:

$$\mathcal{P}_\Delta(x_{t+1} | x_t, a_t) = \mathcal{P}(s_{t-\Delta+1} | s_{t-\Delta}, a_{t-\Delta}) \delta_{a_t}(a'_t) \prod_{i=1}^{\Delta-1} \delta_{a_{t-i}}(a'_{t-i}), \quad (4)$$

where  $\delta$  denotes the Direct delta distribution. Given the augmented state  $x_t$ , the currently unobserved state  $s_t$  can be inferred based on a belief  $b_\Delta(s_t | x_t)$  (Liotet, 2023), representing the probability of  $s_t$  given  $x_t$ , which is formulated as:

$$b_\Delta(s_t | x_t) = \int_{\mathcal{S}^{\Delta-1}} \mathcal{P}(s_t | s_{t-1}, a_{t-1}) \prod_{i=t-\Delta}^{t-2} \mathcal{P}(s_{i+1} | s_i, a_i) ds_{i+1}. \quad (5)$$

Learning this belief enables the agent to infer non-delayed state information and select the timely action. Additionally, since  $s_t$  is not explicitly observed at time  $t$ , the augmented reward is defined as the expectation under this belief:  $\mathcal{R}_\Delta(x_t, a_t) = \mathbb{E}_{b_\Delta(s_t | x_t)} [\mathcal{R}(s_t, a_t)]$ .

### 3.2 Random-Delay MDPs

Following similar arguments as in Katsikopoulos and Engelbrecht (2003), an RDMDP is defined as an eight-tuple  $(\mathcal{S}, \mathcal{A}, \mathcal{P}, \mathcal{R}, \gamma, O, \lambda_o, \tau)$ , where  $O \in \mathbb{Z}_{>0}$  represents a random observation delay, which is sampled from an arbitrary distribution  $\lambda_o$  with supports on the finite integer set  $\{1, 2, \dots, o_{\max}\}$ , with  $o_{\max}$  denoting the maximum allowable delay. The time-indexing function  $\tau : \mathcal{S} \rightarrow \mathbb{N}$  maps each state to the time step at which it becomes available for decision-making.

Under this definition, the augmented states are defined as follows:

**Definition 3.1.** Let  $s_n^{o_n}$  denote the state generated at time  $n > 0$  with an observation delay  $o_n \sim \lambda_o$ , and let  $(a_i)_{i=n}^{t-1}$  denote the sequence of historical actions taken from time  $n$  to  $t-1$ . Suppose that  $s_n^{o_n}$  is the most recent usable state at time step  $t$ . Then, the augmented state is defined as:

$$\hat{x}_t = (s_n^{o_n}, a_n, a_{n+1}, \dots, a_{t-1}), \quad \text{for some } t \in [\tau(s_n^{o_n}), n + o_{\max}] \cap \mathbb{Z}. \quad (6)$$

where the notation  $\hat{\cdot}$  indicates the augmented state defined in RDMDPs.

Assuming that  $\tau(s_n^{o_n}) = t$ , the augmented state at the next time step is defined as:

$$\hat{x}_{t+1} = \begin{cases} (s_{n+1}^{o_{n+1}}, a_{n+1}, a_{n+2}, \dots, a_t) & \text{with } m(o_{n+1}) \\ (s_n^{o_n}, a_n, a_{n+1}, \dots, a_t) & \text{with } 1 - m(o_{n+1}), \end{cases} \quad (7)$$

where  $m(o_{n+1}) = \mathbb{P}(o_{n+1} \in \{1, 2, \dots, \tau(s_n^{o_n}) - n\})$  represents the probability that the next state  $s_{n+1} \sim \mathcal{P}(\cdot | s_n, a_n)$  becomes available by this time. Under the ordering assumption, the state  $s_n$  continues to be used until the subsequent state  $s_{n+1}$  becomes available, at which point the agent switches to use  $s_{n+1}$  to form the augmented state accordingly (see Fig. 1).

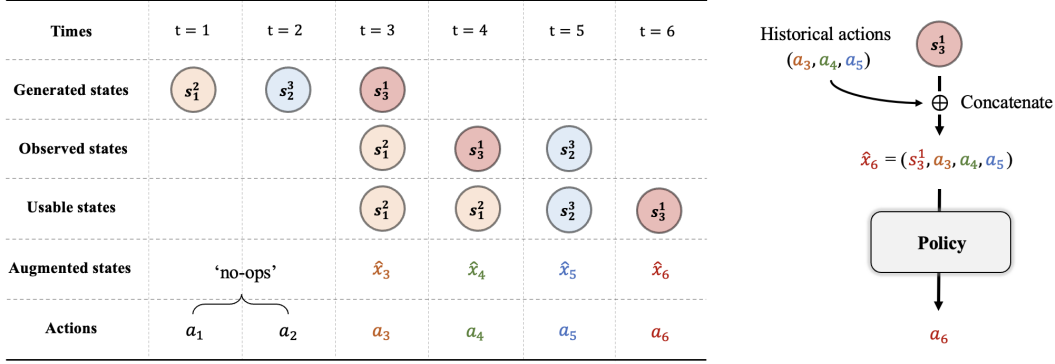


Figure 1: A visual example of the decision-making process in a random-delay environment. At time 3, the state  $s_1^2$  is observed, and the agent can use it to form an augmented state for decision-making. At time 4, the state  $s_3^1$  is observed, while the preceding state  $s_2^3$  remains unobserved. Consequently,  $s_3^1$  cannot be used at this time, as the previously generated state  $s_2^3$  has not yet been used. The agent continues to use  $s_1^2$ . At time 5, the state  $s_2^3$  is observed, and the observed states are then used in order.

## 4 Conservative Agent: Bridging RMDPs and CDMDPs

In this section, we demonstrate how the proposed conservative agent transforms random-delay environments into their constant-delay equivalents. As noted, this approach provides a straightforward plug-in framework that allows any state-of-the-art constant-delay method to be directly applied to random-delay environments without modifications to the algorithmic structure or loss of performance. Ultimately, integrating the conservative agent with the complete information method yields an equivalent delay-free MDP for any random-delay MDP.

### 4.1 Conservative Agent

When delays are bounded and randomly distributed, the proposed agent adopts a conservative strategy that makes decisions on each observed state at its maximum allowable delayed time step. Specifically, for any state  $s_n$  with observation delay  $o_n \sim \lambda_o$ , the conservative agent assumes that the observed state becomes available for decision-making at time  $n + o_{\max}$ , that is:

$$\tau(s_n^{o_n}) = n + o_{\max}, \quad \forall n > 0. \quad (8)$$

Consequently, every state is used exactly  $o_{\max}$  time steps after being generated. This conservative approach provides a simple yet robust solution for decision-making under random delays, eliminating the need to infer or observe the exact delay associated with each state.

For example, suppose the state  $s_1^{o_1}$  is observed at time  $1 + o_1$ . Despite being observed, the conservative agent defers its use until time  $1 + o_{\max}$ . Similarly, the subsequent state  $s_2^{o_2}$  is observed at time  $2 + o_2$ , yet is used only at time  $2 + o_{\max}$ , irrespective of its actual delay.

Formally, for any  $n > 0$ , the augmented state at time  $t = n + o_{\max}$  is defined as:

$$\hat{x}_t = (s_n^{o_n}, a_n, a_{n+1}, \dots, a_{t-1}). \quad (9)$$

Substituting  $n = t - o_{\max}$  yields:

$$\hat{x}_t = (s_{t-o_{\max}}^{o_{t-o_{\max}}}, a_{t-o_{\max}}, a_{t-o_{\max}+1}, \dots, a_{t-1}), \quad \forall t > o_{\max}. \quad (10)$$

This formulation is consistent with the definition of the augmented state in CDMDPs with a constant delay  $\Delta = o_{\max}$ . As previously discussed, this constant-delay formulation can ultimately be reduced to an equivalent delay-free MDP  $(\mathcal{X}, \mathcal{A}, \mathcal{P}_\Delta, \mathcal{R}_\Delta, \gamma)$ .

As a result, the random-delay environment can be reformulated as a constant-delay equivalent with  $\Delta = o_{\max}$  via the conservative agent, thereby enabling direct extension of existing constant-delay methods to random-delay environments without requiring modifications to the algorithmic structure or incurring performance degradation. A visual representation is provided in Fig. 2 and Appendix H.

**Proposition 4.1.** Let  $\lambda_o$  be an arbitrary delay distribution with supports on the finite integer set  $\{1, 2, \dots, o_{\max}\}$ , from which the observation delay  $o_n$  for state  $s_n$  is sampled. Suppose that the agent follows the conservative approach such that, for all  $t > o_{\max}$ , the augmented state is defined as:

$$\hat{x}_t = (s_{t-o_{\max}}^{o_n}, a_{t-o_{\max}}, a_{t-o_{\max}+1}, \dots, a_{t-1}). \quad (11)$$

Then, the random-delay environment can be reformulated as a constant-delay equivalent with delay  $\Delta = o_{\max}$ , which can be further reduced to an equivalent delay-free MDP  $(\mathcal{X}, \mathcal{A}, \mathcal{P}_\Delta, \mathcal{R}_\Delta, \gamma)$ , where  $\Delta$  denotes the constant observation delay.

*Proof.* See Appendix D □

To support our analysis, we present empirical results on Proposition 4.1 in Appendix D, demonstrating that the performance of the conservative agent in random-delay environments is *nearly identical* to that of the normal agent in constant-delay environments with  $\Delta = o_{\max}$ .

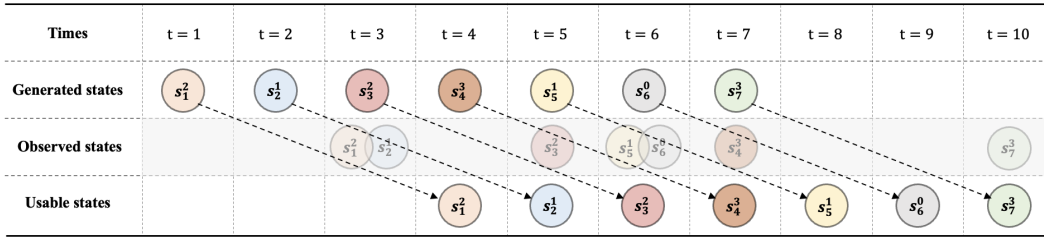


Figure 2: A visual example illustrating the conservative agent-based decision-making process under random delays, where the maximum allowable delay  $o_{\max} = 3$ . Despite state observations occurring simultaneously or being out of chronological order of events, all the delayed states consistently become available for use at their maximum allowable delayed times, i.e.,  $\tau(s_n^{o_n}) = n + o_{\max}, \forall n > 0$ .

## 4.2 Conservative-BPQL

We have shown that, by combining the complete information method with the conservative agent, a random-delay environment can be reformulated as a constant-delay equivalent with  $\Delta = o_{\max}$ , which can subsequently be reduced to an equivalent delay-free MDP. While the complete information method offers a solid theoretical foundation for learning policies in delay-free MDPs, it often suffers from a state space explosion, where the state space grows exponentially with the degree of delay, as  $\mathcal{X} = \mathcal{S} \times \mathcal{A}^\Delta$ , often resulting in extreme sample inefficiency and slow learning (Derman et al., 2021).

To alleviate this limitation, we integrate the conservative agent into the BPQL framework (Kim et al., 2023), which is specifically designed to handle constant delays while effectively mitigating the state-space explosion problem and has demonstrated strong empirical performance. This integration yields the conservative-BPQL algorithm, which is summarized in Algorithm 1.

More specifically, BPQL is an actor-critic algorithm that learns the critic using an approximate value function over augmented state, termed the beta-value function, defined as:

$$\tilde{Q}^{\pi_\Delta}(\hat{x}_t, a_t) = \mathbb{E}_{b_\Delta(s_t|\hat{x}_t)} \left[ Q_\beta^{\pi_\Delta}(s_t, a_t) \right] + \zeta^{\pi_\Delta}(\hat{x}_t, a_t), \quad (12)$$

where  $\tilde{Q}^{\pi_\Delta}$  and  $Q_\beta^{\pi_\Delta}$  denote the augmented state-based  $Q$ -value and the beta  $Q$ -value, respectively, and  $\zeta^{\pi_\Delta}$  represents the projection residual. Notably,  $Q_\beta^{\pi_\Delta}$  is evaluated with respect to the original state space rather than the augmented one, thereby inherently mitigating the learning inefficiencies associated with state space explosion.

In particular, the beta  $Q$ -value and the augmented state-based policy  $\pi_\Delta$  are parameterized by  $\theta$  (beta-critic) and  $\phi$  (actor), respectively. These parameters are updated iteratively to minimize the

following objective functions; for the beta-critic:

$$\begin{aligned} \mathcal{J}_{Q_\beta}(\theta) = & \mathbb{E}_{(s_t, a_t, r_t, s_{t+1}, \hat{x}_{t+1}) \sim \mathcal{D}} \left[ \frac{1}{2} \left( Q_{\theta, \beta}^{\pi_\phi}(s_t, a_t) - \mathcal{R}(s_t, a_t) \right. \right. \\ & \left. \left. - \gamma \mathbb{E}_{a_{t+1} \sim \pi_\phi} \left[ Q_{\tilde{\theta}, \beta}^{\pi_\phi}(s_{t+1}, a_{t+1}) - \alpha \log \pi_\phi(a_{t+1} \mid \hat{x}_{t+1}) \right] \right)^2 \right] \end{aligned} \quad (13)$$

and for the actor:

$$\mathcal{J}_\pi(\phi) = \mathbb{E}_{(s_t, \hat{x}_t) \sim \mathcal{D}} \left[ \mathbb{E}_{a_t \sim \pi_\phi} \left[ \alpha \log \pi_\phi(a_t \mid \hat{x}_t) - Q_{\theta, \beta}^{\pi_\phi}(s_t, a_t) \right] \right], \quad (14)$$

where  $\mathcal{D}$  represents a replay buffer (Mnih et al., 2013),  $\alpha$  is a temperature (Haarnoja et al., 2018), and  $\tilde{\theta}$  are the parameters of the target beta-critic (Fujimoto et al., 2018).

It is worth note that while we specifically instantiate the conservative agent into the BPQL framework, any constant-delay method can be extended to random-delay environments with the aid of this agent. To demonstrate this generality, we investigate a second conservative agent-based algorithm, termed conservative-VDPO, which builds upon another state-of-the-art constant-delay method, variational delayed policy optimization (Wu et al., 2024a). The corresponding results are presented in section 5.3.

## 5 Experiments

### 5.1 Benchmarks and Baseline Algorithms

We evaluated the conservative agent-based algorithm on continuous control tasks in the MuJoCo benchmark under different maximum allowable delays,  $o_{\max} \in \{5, 10, 20\}$ , to assess its performance and robustness with respect to the degree of randomness in delays. Throughout all experiments, we assumed  $\lambda_o$  to be an uniform distribution. Details of the benchmark environments and experimental setup are provided in Appendix A.

The following algorithms were included as baselines in the experiments: SAC (Haarnoja et al., 2018), delayed-SAC (Derman et al., 2021), DC/AC (Bouteiller et al., 2020), and state augmentation-MLP (Wang et al., 2023). The normal SAC serves as a naive baseline that selects actions for currently usable states in a memoryless basis and performs ‘no-ops’ otherwise, without concerning the violation of the Markov assumption. Delayed-SAC is a variant of delayed- $Q$  (Derman et al., 2021), adapted by Kim et al. (2023) for continuous spaces. It constructs an approximate dynamics model to infer unobserved states through recursive one-step predictions repeated over the delayed time steps. DC/AC is another variant of SAC that incorporates off-policy multi-step value estimation with a partial trajectory resampling strategy, significantly improving sample efficiency and demonstrating remarkable performance under random delays. Lastly, state augmentation-MLP is a most recent algorithm that leverages time-calibrated information obtained from offline datasets to train its critic. Combined with auxiliary techniques, it has shown strong empirical performance under random delays.

### 5.2 Results

Table 1 and Fig. 3 present the performance of each algorithm on the MuJoCo benchmarks. Empirical results reveal that the proposed conservative-BPQL demonstrates the most remarkable performance across all tasks. In contrast, SAC, which does not account for the effect of delays, exhibits performance comparable to that of a random policy. Despite respectable performance in tasks with relatively small state spaces, delayed-SAC exhibits inconsistent and task-dependent performance overall. This may be attributed to the accumulation of prediction errors as task complexity or the degree of randomness in delay increases, underscoring the need for a more carefully designed dynamics model. Lastly, while DC/AC and state augmentation-MLP perform reasonably well under short maximum allowable delays, their effectiveness significantly deteriorates as  $o_{\max}$  increases.

Moreover, the results in Table 1 confirm that the performance of the conservative agent in random-delay environments (conservative-BPQL) is *nearly identical* to that of the normal agent in constant-delay environments with  $\Delta = o_{\max}$  (BPQL) across all tasks. This strongly supports our argument that random-delay environments can be reformulated as constant-delay equivalents with the aid of the conservative agent. Additional results are provided in Appendix C.1 and Appendix D.1.

Table 1: Results on the MuJoCo benchmarks with random delays  $o_{\max} \in \{5, 10, 20\}$ . Each algorithm was evaluated for one million time steps with five different seeds, where the standard deviations of average returns are denoted by  $\pm$ . The best performances are colored in **blue** and the results under constant delay  $\Delta = o_{\max}$  are colored in **red**. Delay-free SAC serves as the delay-free baseline.

Environment		Ant-v3	HalfCheetah-v3	Hopper-v3	Walker2d-v3	Humanoid-v3	InvertedPendulum-v2
$o_{\max}$	Algorithm						
×	Random policy	-58.7 $\pm$ 4	-285.01 $\pm$ 3	18.6 $\pm$ 2	1.9 $\pm$ 1	121.9 $\pm$ 2	5.6 $\pm$ 1
	Delay-free SAC	3279.2 $\pm$ 180	8608.4 $\pm$ 57	2435.2 $\pm$ 23	3305.5 $\pm$ 234	3228.1 $\pm$ 410	964.3 $\pm$ 29
5	SAC	-76.6 $\pm$ 4	-279.5 $\pm$ 5	89.2 $\pm$ 10	44.7 $\pm$ 21	403.9 $\pm$ 5	32.2 $\pm$ 2
	DC/AC	907.5 $\pm$ 90	2561.8 $\pm$ 92	1931.6 $\pm$ 192	2079.3 $\pm$ 122	2798.4 $\pm$ 452	854.7 $\pm$ 30
	Delayed-SAC	986.4 $\pm$ 128	4569.4 $\pm$ 88	<b>2200.4<math>\pm</math>190</b>	1910.1 $\pm$ 247	418.9 $\pm$ 126	<b>964.2<math>\pm</math>15</b>
	State Augmentation-MLP	916.1 $\pm$ 621	2442.1 $\pm$ 79	1946.1 $\pm$ 144	2144.8 $\pm$ 361	493.3 $\pm$ 18	283.1 $\pm$ 27
	Conservative-BPQL (ours)	<b>3679.8<math>\pm</math>167</b>	<b>5583.9<math>\pm</math>169</b>	2174.1 $\pm$ 155	<b>2843.2<math>\pm</math>272</b>	<b>3157.7<math>\pm</math>292</b>	958.8 $\pm$ 14
	BPQL (constant)	<b>3761.9<math>\pm</math>112</b>	<b>5212.7<math>\pm</math>41</b>	<b>2136.3<math>\pm</math>158</b>	<b>2577.4<math>\pm</math>157</b>	<b>3194.9<math>\pm</math>374</b>	<b>955.9<math>\pm</math>28</b>
10	SAC	-84.6 $\pm$ 9	-278.6 $\pm$ 6	28.1 $\pm$ 6	40.9 $\pm$ 4	354.5 $\pm$ 12	31.3 $\pm$ 1
	DC/AC	342.9 $\pm$ 34	1824.5 $\pm$ 111	1262.4 $\pm$ 261	1492.5 $\pm$ 133	1023.8 $\pm$ 359	4.9 $\pm$ 0
	Delayed-SAC	966.9 $\pm$ 180	2563.8 $\pm$ 215	1878.5 $\pm$ 176	1264.6 $\pm$ 233	289.6 $\pm$ 108	<b>947.6<math>\pm</math>36</b>
	State Augmentation-MLP	779.4 $\pm$ 554	1926.3 $\pm$ 197	1286.7 $\pm$ 124	1148.3 $\pm$ 283	470.3 $\pm$ 11	58.7 $\pm$ 4
	Conservative-BPQL (ours)	<b>2744.5<math>\pm</math>112</b>	<b>4810.1<math>\pm</math>233</b>	<b>2300.9<math>\pm</math>164</b>	<b>2122.3<math>\pm</math>292</b>	<b>2820.5<math>\pm</math>348</b>	936.9 $\pm$ 38
	BPQL (constant)	<b>2831.9<math>\pm</math>103</b>	<b>4282.2<math>\pm</math>203</b>	<b>2129.2<math>\pm</math>184</b>	<b>2331.6<math>\pm</math>252</b>	<b>2891.5<math>\pm</math>357</b>	<b>934.7<math>\pm</math>20</b>
20	SAC	-83.1 $\pm$ 9	-264.9 $\pm$ 5	27.5 $\pm$ 5	64.6 $\pm$ 1	364.3 $\pm$ 7	24.3 $\pm$ 0
	DC/AC	258.3 $\pm$ 42	860.9 $\pm$ 288	12.8 $\pm$ 6	-2.9 $\pm$ 5	237.3 $\pm$ 73	4.1 $\pm$ 0
	Delayed-SAC	955.7 $\pm$ 110	1377.8 $\pm$ 140	1164.1 $\pm$ 278	811.5 $\pm$ 163	370.3 $\pm$ 17	<b>933.5<math>\pm</math>33</b>
	State Augmentation-MLP	748.8 $\pm$ 506	915.1 $\pm$ 101	488.7 $\pm$ 54	442.2 $\pm$ 191	455.7 $\pm$ 6	24.3 $\pm$ 1
	Conservative-BPQL (ours)	<b>1976.5<math>\pm</math>248</b>	<b>3727.2<math>\pm</math>279</b>	<b>1346.7<math>\pm</math>245</b>	<b>1025.7<math>\pm</math>302</b>	<b>1143.8<math>\pm</math>371</b>	566.9 $\pm$ 88
	BPQL (constant)	<b>2078.9<math>\pm</math>157</b>	<b>3062.7<math>\pm</math>252</b>	<b>1526.7<math>\pm</math>227</b>	<b>846.7<math>\pm</math>443</b>	<b>1197.7<math>\pm</math>457</b>	<b>608.7<math>\pm</math>210</b>

### 5.3 Ablation Study

#### 5.3.1 Conservative-VDPO

As aforementioned, any constant-delay method can be extended to random-delay environments via the conservative agent. To demonstrate this generality, we investigated a second conservative agent-based algorithm, termed conservative-VDPO, which builds upon another state-of-the-art constant-delay method, variational delayed policy optimization (VDPO) (Wu et al., 2024a), without any modification to the original algorithmic structure. The corresponding results are provided in Table 2.

The results show that both conservative agent-based algorithms exhibit strong empirical performance. Given that the BPQL and VDPO algorithms were not originally designed to operate under random delays, these findings clearly highlight the efficacy and broad applicability of the conservative agent, suggesting great potential for further improvement as constant-delay methods continue to evolve.

#### 5.3.2 Causality in Observations

Under random observation delays, the observation times of states are often scrambled, disrupting the identification of causal relationships between them. Since both complete information methods and model-based approaches rely heavily on understanding these relationships to infer non-delayed information, it becomes challenging for agents to make accurate decisions under random delays.

To examine the effect of disrupted causality in observations, we conducted an experiment comparing the performance of agents that make decisions based on the observed order (unordered agent) versus the generated order of states (ordered agent). The corresponding results are presented in Appendix E.

The results reveal that preserving causal consistency in observations significantly affects both the performance and learning stability of RL agents, with performance degradation becoming more

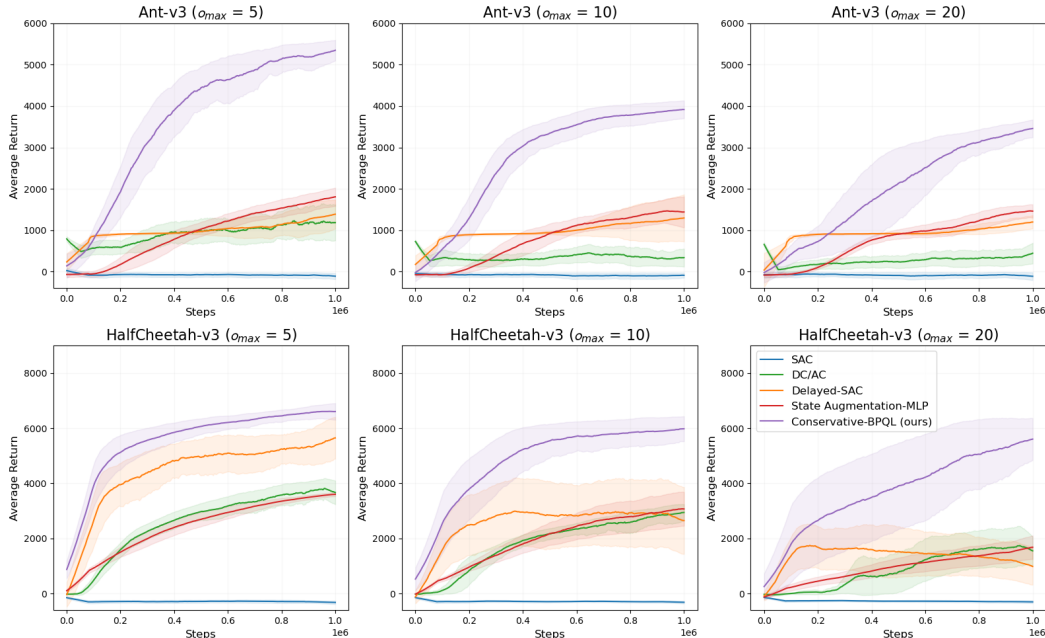


Figure 3: Performance curves of the baseline algorithms on continuous control tasks in the MuJoCo benchmark with random delays  $o_{\max} \in \{5, 10, 20\}$ . All tasks were conducted with five different seeds for one million time steps, and the shaded regions represent the standard deviation of average returns. Across all tasks, the proposed conservative-BPQL demonstrates the most remarkable performance.

Table 2: Results of the conservative agent-based algorithms evaluated for one million time steps with five different seeds, with the standard deviations of average returns denoted by  $\pm$ .

Environment		Ant-v3	HalfCheetah-v3	Hopper-v3	Walker2d-v3	Humanoid-v3	InvertedPendulum-v2
$o_{\max}$	Algorithm						
5	Conservative-BPQL (ours)	3679.8 $\pm$ 167	5583.9 $\pm$ 169	2174.1 $\pm$ 155	2843.2 $\pm$ 272	3157.7 $\pm$ 292	958.8 $\pm$ 14
	Conservative-VDPO (ours)	4373.3 $\pm$ 181	4871.9 $\pm$ 41	1942.1 $\pm$ 115	3415.7 $\pm$ 283	2845.2 $\pm$ 515	774.2 $\pm$ 136
10	Conservative-BPQL (ours)	2744.5 $\pm$ 112	4810.1 $\pm$ 233	2300.9 $\pm$ 164	2122.3 $\pm$ 292	2820.5 $\pm$ 348	936.9 $\pm$ 38
	Conservative-VDPO (ours)	3086.2 $\pm$ 106	3355.5 $\pm$ 210	1952.3 $\pm$ 114	2608.2 $\pm$ 235	2189.4 $\pm$ 474	610.9 $\pm$ 114
20	Conservative-BPQL (ours)	1976.5 $\pm$ 248	3727.2 $\pm$ 279	1346.7 $\pm$ 245	1025.7 $\pm$ 302	1143.8 $\pm$ 371	566.9 $\pm$ 88
	Conservative-VDPO (ours)	2419.7 $\pm$ 95	2364.9 $\pm$ 180	1366.2 $\pm$ 186	804.8 $\pm$ 129	996.5 $\pm$ 90	19.4 $\pm$ 8

pronounced as randomness in delays increases. Note that the conservative agent is systematically unaffected by this issue, as it consistently uses temporally appropriate states in their generated order.

## 6 Conclusion

In this study, we investigated environments with random delays and proposed a *conservative agent* for robust decision-making under such conditions. This agent provides a straightforward plug-in framework that transforms a random-delay environment into its constant-delay equivalent, thereby enabling any state-of-the-art constant-delay method to be directly extended to random-delay environments, without requiring algorithmic modification or sacrificing performance. Ultimately, integrating the conservative agent with the complete information method yields a delay-free equivalent for any random-delay environment.

Empirical results demonstrate that the conservative agent-based algorithms consistently outperform existing baseline algorithms in terms of both asymptotic performance and sample efficiency under random delays. We believe this agent allows researchers to avoid treating constant-delay and random-

delay environments as separate problems, thereby facilitating more focused and in-depth research in the field of delayed RL.

## 7 Related Work

Delays are prevalent in real-world RL applications due to factors such as computational time and network latency. Prior research on addressing such delays within the RL framework can be categorized into two main branches: the complete information method and the model-based approach.

**Complete information method** The complete information method is often favored in delayed environments as it can restore the Markov property (Katsikopoulos and Engelbrecht, 2003), thereby allowing policy learning through conventional RL algorithms. Despite its solid theoretical foundation, the augmentation of the state space introduces challenges related to sample complexity.

To address this limitation, Bouteiller et al. (2020) proposes a variant of SAC that combines off-policy multi-step value estimation with a partial trajectory resampling strategy, significantly enhancing sample efficiency. Kim et al. (2023) introduces an alternative representation for augmented values, which are evaluated with respect to the original state space rather than the augmented one, inherently mitigating sample inefficiencies. More recently, Wu et al. (2024b) alleviates performance degradation caused by this issue by leveraging auxiliary tasks with shorter delays to assist learning in tasks with longer delays. Wang et al. (2023) adopts another approach that uses offline datasets to obtain time-calibrated, non-delayed information, effectively avoiding the issue of sample complexity. Wu et al. (2024a) formulates delayed RL as a variational inference problem and proposes an iterative approach that learns a delay-free policy and distills it into delayed environments through behavior cloning, achieving high sample efficiency.

**Model-Based Approach** The model-based approach seeks to restore the Markov property by learning the underlying delay-free environmental dynamics (Walsh et al., 2009; Firoiu et al., 2018; Chen et al., 2021; Derman et al., 2021). For example, Derman et al. (2021) constructs an approximate dynamics model from transition samples collected in a delay-free environment and employs it in a delayed environment to infer non-delayed information through recursive one-step predictions. Similarly, Firoiu et al. (2018) utilizes recurrent neural networks (Cho, 2014) to model temporal dynamics. These approaches facilitate more sample-efficient learning by avoiding the sample complexity issues introduced by state augmentation. However, their strong reliance on accuracy dynamics modeling makes them vulnerable to model inaccuracies; even slight prediction errors can be accumulated over recursion, which may severely degrade policy performance.

While numerous delay-compensating methods have demonstrated their promise, most studies have either assumed constant delays or required explicit knowledge of individual delay durations. These assumptions limit their applicability to more realistic settings involving random delays with unknown characteristics. Motivated by the impressive performance of state-of-the-art constant-delay methods, this study makes its primary contribution by proposing a straightforward plug-in framework based on a conservative agent. This agent transforms a random-delay environment into its constant-delay equivalent, thereby enabling the direct application of any constant-delay method to random-delay environments, without requiring algorithmic modifications or incurring performance degradation.

## References

- Abadía, I., Naveros, F., Ros, E., Carrillo, R. R., and Luque, N. R. (2021). A cerebellar-based solution to the nondeterministic time delay problem in robotic control. *Science Robotics*, 6(58):eabf2756.
- Altman, E. and Nain, P. (1992). Closed-loop control with delayed information. *ACM Sigmetrics Performance Evaluation Review*, 20(1):193–204.
- Bellman, R. (1957). A markovian decision process. *Journal of Mathematics and Mechanics*, pages 679–684.
- Bouteiller, Y., Ramstedt, S., Beltrame, G., Pal, C., and Binas, J. (2020). Reinforcement learning with random delays. In *International Conference on Learning Representations*.
- Chen, B., Xu, M., Li, L., and Zhao, D. (2021). Delay-aware model-based reinforcement learning for continuous control. *Neurocomputing*, 450:119–128.

- Cho, K. (2014). Learning phrase representations using RNN encoder-decoder for statistical machine translation. *arXiv preprint arXiv:1406.1078*.
- Derman, E., Dalal, G., and Mannor, S. (2021). Acting in delayed environments with non-stationary Markov policies. *arXiv preprint arXiv:2101.11992*.
- Firoiu, V., Ju, T., and Tenenbaum, J. (2018). At human speed: deep reinforcement learning with action delay. *arXiv preprint arXiv:1810.07286*.
- Fujimoto, S., Hoof, H., and Meger, D. (2018). Addressing function approximation error in actor-critic methods. In *International Conference on Machine Learning*, pages 1587–1596. PMLR.
- Ge, Y., Chen, Q., Jiang, M., and Huang, Y. (2013). Modeling of random delays in networked control systems. *Journal of Control Science and Engineering*, 2013(1):383415.
- Haarnoja, T., Zhou, A., Hartikainen, K., Tucker, G., Ha, S., Tan, J., Kumar, V., Zhu, H., Gupta, A., Abbeel, P., et al. (2018). Soft actor-critic algorithms and applications. *arXiv preprint arXiv:1812.05905*.
- Hwangbo, J., Sa, I., Siegwart, R., and Hutter, M. (2017). Control of a quadrotor with reinforcement learning. *IEEE Robotics and Automation Letters*, 2(4):2096–2103.
- Kalashnikov, D., Irpan, A., Pastor, P., Ibarz, J., Herzog, A., Jang, E., Quillen, D., Holly, E., Kalakrishnan, M., Vanhoucke, V., et al. (2018). Scalable deep reinforcement learning for vision-based robotic manipulation. In *Conference on Robot Learning*, pages 651–673. PMLR.
- Katsikopoulos, K. V. and Engelbrecht, S. E. (2003). Markov decision processes with delays and asynchronous cost collection. *IEEE Transactions on Automatic Control*, 48(4):568–574.
- Kim, J., Kim, H., Kang, J., Baek, J., and Han, S. (2023). Belief projection-based reinforcement learning for environments with delayed feedback. *Advances in Neural Information Processing Systems*, 36:678–696.
- Kingma, D. P. (2014). Adam: A method for stochastic optimization. *arXiv preprint arXiv:1412.6980*.
- Liotet, P. (2023). Delays in reinforcement learning. *arXiv preprint arXiv:2309.11096*.
- Liotet, P., Maran, D., Bisi, L., and Restelli, M. (2022). Delayed reinforcement learning by imitation. In *International Conference on Machine Learning*, pages 13528–13556. PMLR.
- Mahmood, A. R., Korenkevych, D., Komer, B. J., and Bergstra, J. (2018). Setting up a reinforcement learning task with a real-world robot. In *2018 IEEE/RSJ International Conference on Intelligent Robots and Systems (IROS)*, pages 4635–4640. IEEE.
- Mnih, V., Kavukcuoglu, K., Silver, D., Graves, A., Antonoglou, I., Wierstra, D., and Riedmiller, M. (2013). Playing atari with deep reinforcement learning. *arXiv preprint arXiv:1312.5602*.
- Silver, D., Huang, A., Maddison, C. J., Guez, A., Sifre, L., Van Den Driessche, G., Schrittwieser, J., Antonoglou, I., Panneershelvam, V., Lanctot, M., et al. (2016). Mastering the game of Go with deep neural networks and tree search. *Nature*, 529(7587):484–489.
- Singh, S. P., Jaakkola, T., and Jordan, M. I. (1994). Learning without state-estimation in partially observable Markovian decision processes. In *Machine Learning Proceedings 1994*, pages 284–292. Elsevier.
- Todorov, E., Erez, T., and Tassa, Y. (2012). Mujoco: A physics engine for model-based control. In *2012 IEEE/RSJ International Conference on Intelligent Robots and Systems*, pages 5026–5033. IEEE.
- Walsh, T. J., Nouri, A., Li, L., and Littman, M. L. (2009). Learning and planning in environments with delayed feedback. *Autonomous Agents and Multi-Agent Systems*, 18:83–105.
- Wang, W., Han, D., Luo, X., and Li, D. (2023). Addressing signal delay in deep reinforcement learning. In *The Twelfth International Conference on Learning Representations*.
- Wu, Q., Zhan, S. S., Wang, Y., Wang, Y., Lin, C.-W., Lv, C., Zhu, Q., and Huang, C. (2024a). Variational delayed policy optimization. *Advances in Neural Information Processing Systems*, 37:54330–54356.
- Wu, Q., Zhan, S. S., Wang, Y., Wang, Y., Lin, C.-W., Lv, C., Zhu, Q., Schmidhuber, J., and Huang, C. (2024b). Boosting reinforcement learning with strongly delayed feedback through auxiliary short delays. In *International Conference on Machine Learning*, pages 53973–53998. PMLR.

## A Experimental details

### A.1 Environmental details

Table 3: Environmental details of the MuJoCo benchmark.

Environment	State dimension	Action dimension	Time step (s)
Ant-v3	27	8	0.05
HalfCheetah-v3	17	6	0.05
Walker2d-v3	17	6	0.008
Hopper-v3	11	3	0.008
Humanoid-v3	376	17	0.015
InvertedPendulum-v2	4	1	0.04

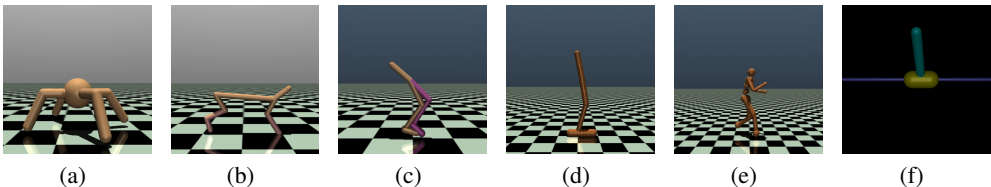


Figure 4: Experimental environments in the MuJoCo benchmark: (a) Ant-v3 (b) HalfCheetah-v3, (c) Walker2d-v3, (d) Hopper-v3, (e) Humanoid-v3, and (f) InvertedPendulum-v2

### A.2 Implementation details

The implementation details of the conservative-BPQL align with those presented in Kim et al. (2023), with the specific hyperparameters listed in Table 4. Since the baseline algorithms included in our experiments employ the SAC algorithm as their foundational learning algorithm, the hyperparameters are consistent across all approaches, except for the DC/AC and state augmentation-MLP algorithms, which were implemented with the source code provided by its authors.

Table 4: Hyperparameters for the baseline algorithms.

Hyperparameters	Values
Actor network	256, 256
Critic network	256, 256
Learning rate (actor)	3e-4
Learning rate (beta-critic)	3e-4
Temperature ( $\alpha$ )	0.2
Discount factor ( $\gamma$ )	0.99
Replay buffer size	1e6
Mini-Batch size	256
Target entropy	$-\dim \mathcal{A} $
Target smoothing coefficient ( $\xi$ )	0.995
Optimizer	Adam (Kingma, 2014)
Total time steps	1e6

## B Pseudo code of Conservative-BPQL

The proposed conservative agent can be seamlessly integrated into the BPQL framework with minimal modifications by deferring decision-making on the initial state until its maximum allowable delayed time step. Subsequently, all states become available for use in order.

In the implementation, a temporary buffer  $\mathcal{B}$  has been employed as in Kim et al. (2023) to store the observed states, corresponding rewards, and historical actions, which enables the agent to access timely and delay-relevant historical information for constructing augmented states. Additionally, we assumed that the reward feedback is also maximally delayed in equivalent constant-delay environments, thereby the reward corresponding to the action  $a_t$  is assumed to be  $r_{t-o_{\max}}$ .

---

### Algorithm 1 Conservative Belief Projection-based $Q$ -Learning (Conservative-BPQL)

---

**Input:** actor  $\pi_\phi(a|\hat{x})$ , beta-critic  $Q_{\theta,\beta}(s, a)$ , target beta critic  $Q_{\hat{\theta},\beta}(s, a)$ , replay buffer  $\mathcal{D}$ , temporary buffer  $\mathcal{B}$ , maximum delay  $o_{\max}$ , beta-critic learning rate  $\psi_Q$ , actor learning rate  $\psi_\pi$ , soft update rate  $\xi$ , episodic length  $H$ , and total number of episodes  $E$ .

**for** episode  $e = 1$  to  $E$  **do**

**for** time step  $t = 1$  to  $H$  **do**

**if**  $t < o_{\max}$  **then**

      select random or ‘no-ops’ action  $a_t$

      execute  $a_t$  on environment

      put  $a_t$ , observed states, rewards to  $\mathcal{B}$

**else if**  $t = o_{\max}$  **then** ▷ Wait for  $o_{\max}$  time-steps

      select random or ‘no-ops’ action  $a_t$

      execute  $a_t$  on environment

      put  $a_t$ , observed states, rewards to  $\mathcal{B}$

**else**

      get  $s_{t-o_{\max}}, a_{t-o_{\max}}, \dots, a_{t-1}$  from  $\mathcal{B}$

$\hat{x}_t \leftarrow (s_{t-o_{\max}}, a_{t-o_{\max}}, \dots, a_{t-1})$  ▷ Construct augmented state

$a_t \leftarrow \pi_\phi(\hat{x}_t)$

      execute  $a_t$  on environment

      put  $a_t$ , observed states, rewards to  $\mathcal{B}$

**if**  $t > 2o_{\max}$  **then**

        get  $s_{t-2o_{\max}}, s_{t-2o_{\max}+1}, s_{t-o_{\max}}, r_{t-o_{\max}}, a_{t-2o_{\max}}, \dots, a_{t-o_{\max}}$  from  $\mathcal{B}$

$\hat{x}_{t-o_{\max}} \leftarrow (s_{t-2o_{\max}}, a_{t-2o_{\max}}, \dots, a_{t-o_{\max}})$

$\hat{x}_{t-o_{\max}+1} \leftarrow (s_{t-2o_{\max}+1}, a_{t-2o_{\max}+1}, \dots, a_{t-o_{\max}+1})$

        store  $(\hat{x}_{t-o_{\max}}, s_{t-o_{\max}}, a_{t-o_{\max}}, r_{t-o_{\max}}, \hat{x}_{t-o_{\max}+1}, s_{t-o_{\max}+1})$  in  $\mathcal{D}$

        pop  $s_{t-2o_{\max}}, a_{t-2o_{\max}}$  from  $\mathcal{B}$

**end if**

**end if**

**end for**

**for** each gradient step **do**

$\theta \leftarrow \theta - \psi_Q \nabla \mathcal{J}_{Q_\beta}(\theta)$  ▷ Update beta-critic

$\phi \leftarrow \phi - \psi_\pi \nabla \mathcal{J}_\pi(\phi)$  ▷ Update actor

$\hat{\theta} \leftarrow \xi \theta + (1 - \xi) \hat{\theta}$  ▷ Update target beta-critic

**end for**

**Output:** actor  $\pi_\phi$

---

Note that the augmented reward is a random variable that has to be determined based on the conditional expectation as discussed in section 3.1. This expected value can be empirically obtained through the use of replay buffer  $\mathcal{D}$ :

$$\mathcal{R}_\Delta(\hat{x}_{t-o_{\max}}, a_{t-o_{\max}}) \approx \mathbb{E}_{\mathcal{D}}[\mathcal{R}(s_{t-o_{\max}}, a_{t-o_{\max}})]. \quad (15)$$

Consequently, training the beta-critic and actor requires only the following set of experience tuples:

$$(\hat{x}_{t-o_{\max}}, s_{t-o_{\max}}, a_{t-o_{\max}}, r_{t-o_{\max}}, \hat{x}_{t-o_{\max}+1}, s_{t-o_{\max}+1}). \quad (16)$$

## C Experimental Results

### C.1 Performance comparison

**Performance curves** We present the performance curves of each algorithm evaluated on the MuJoCo tasks with random delays  $o_{\max} \in \{5, 10, 20\}$ . All tasks were conducted with five different seeds for one million time steps, where the shaded regions represent the standard deviation of average returns. Empirical results demonstrate that conservative-BPQL exhibits the most remarkable performance across all evaluated tasks.

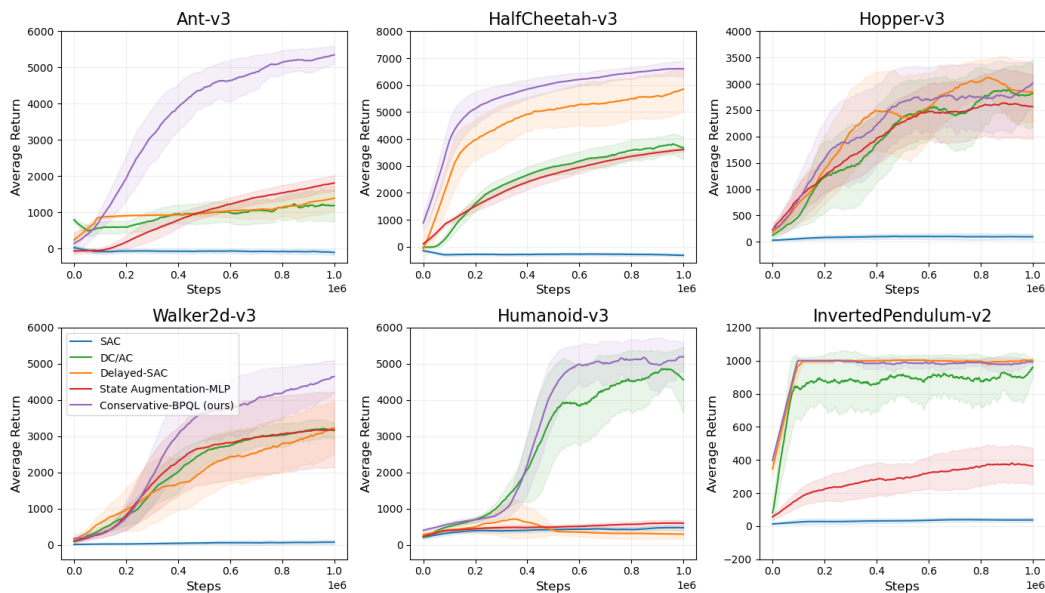


Figure 5: Performance curves of each algorithm on the MuJoCo tasks with  $o_{\max} = 5$ .

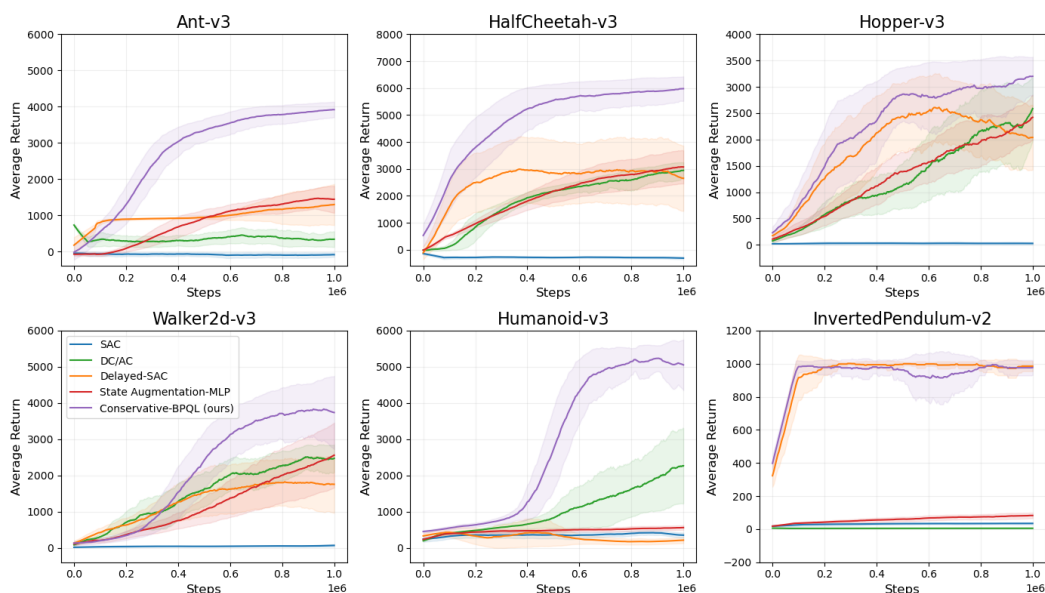


Figure 6: Performance curves of each algorithm on the MuJoCo tasks with  $o_{\max} = 10$ .

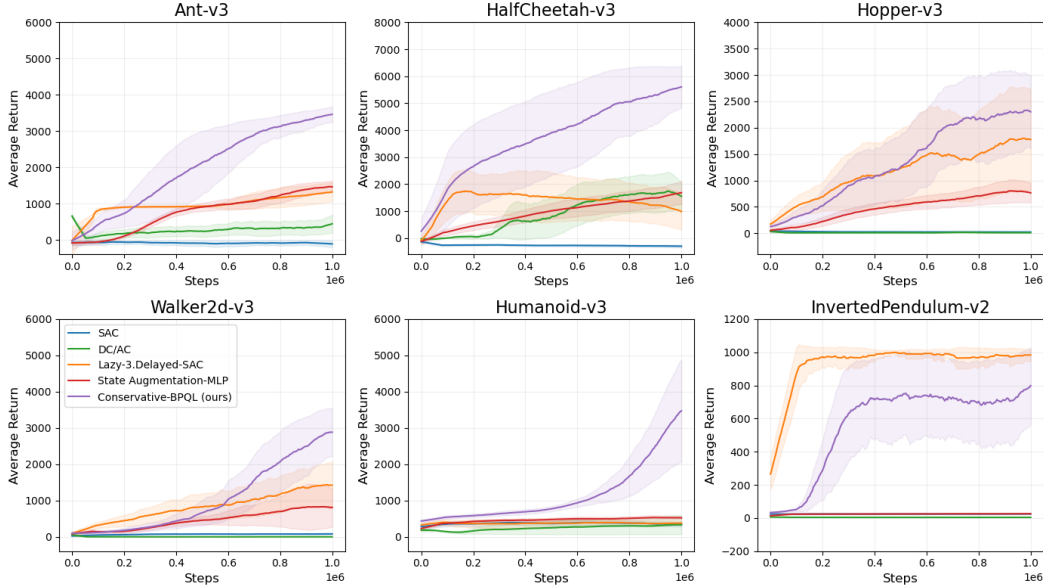


Figure 7: Performance curves of each algorithm on the MuJoCo tasks with  $o_{\max} = 20$ .

**Delay-free normalized scores** To clarify the performance achieved by the conservative agent-based algorithm, we report the delay-free normalized scores in Table 5, which is defined as:

$$R_{\text{normalized}} = (R_{\text{algorithm}} - R_{\text{random}}) / (R_{\text{delay-free}} - R_{\text{random}}), \quad (17)$$

where  $R_{\text{algorithm}}$ ,  $R_{\text{delay-free}}$ , and  $R_{\text{random}}$  represent the average returns of the algorithms, delay-free SAC, and random policy, respectively.

The results confirm that for tasks with  $o_{\max} = \{5, 10\}$ , conservative-BPQL achieves the best performance, with average scores of 0.91 and 0.81, respectively. It outperforms the second-best baseline by wide average margins of 0.28 and 0.34 points. Even for tasks with maximum allowable delay  $o_{\max} = 20$ , conservative-BPQL maintains the highest average score of 0.48, highlighting its strong empirical performance compared to other baseline algorithms.

Table 5: The delay-free normalized scores of the baseline algorithms under random delays. The best scores are highlighted in **bold**.

Environment		Ant-v3	HalfCheetah-v3	Hopper-v3	Walker2d-v3	Humanoid-v3	InvertedPendulum-v2	Average
$o_{\max}$	Algorithm							
5	DC/AC	0.28	0.32	0.79	0.62	0.86	0.88	0.63
	Delayed-SAC	0.31	0.54	0.90	0.57	0.09	<b>1.01</b>	0.57
	State Augmentation-MLP	0.29	0.31	0.80	0.65	0.12	0.29	0.41
	Conservative-BPQL (ours)	<b>1.12</b>	<b>0.68</b>	<b>0.89</b>	<b>0.85</b>	<b>0.97</b>	0.99	<b>0.91</b>
10	DC/AC	0.11	0.23	0.51	0.45	0.29	-0.01	0.26
	Delayed-SAC	0.30	0.32	0.77	0.38	0.05	<b>0.99</b>	0.47
	State Augmentation-MLP	0.25	0.24	0.53	0.34	0.11	0.05	0.25
	Conservative-BPQL (ours)	<b>0.84</b>	<b>0.57</b>	<b>0.94</b>	<b>0.64</b>	<b>0.87</b>	0.98	<b>0.81</b>
20	DC/AC	0.09	0.12	-0.01	0.00	0.04	-0.01	0.03
	Delayed-SAC	0.30	0.18	0.48	0.24	0.08	<b>0.97</b>	0.37
	State Augmentation-MLP	0.24	0.13	0.19	0.13	0.10	0.02	0.14
	Conservative-BPQL (ours)	<b>0.61</b>	<b>0.45</b>	<b>0.55</b>	<b>0.30</b>	<b>0.32</b>	0.58	<b>0.48</b>

## D Proof of Proposition 4.1

In this section, we sketch the proof for Proposition 4.1 stated in the main text.

*Proof sketch.* Let  $\tau : \mathcal{S} \rightarrow \mathbb{N}$  be a time-indexing function that maps each state to the time at which it becomes available for decision-making, and let  $\lambda_o$  be an arbitrary delay distribution supported on the finite integer set  $\{1, 2, \dots, o_{\max}\}$ , from which an observation delay  $o_n$  for state  $s_n$  is sampled.

Suppose the agent follows a conservative approach, making decisions on each observed state  $s_n$  at its maximum allowable delayed time step. Specifically, the agent assumes:

$$\tau(s_n^{o_n}) = n + o_{\max}, \quad \forall n > 0. \quad (18)$$

Under this assumption, the augmented state at time  $t = n + o_{\max}$  is given by:

$$\hat{x}_t = (s_n^{o_n}, a_n, a_{n+1}, \dots, a_{t-1}), \quad (19)$$

and the probability that the next state  $s_{n+1} \sim \mathcal{P}(\cdot | s_n, a_n)$  becomes available by time  $t + 1$  is:

$$m(o_{n+1}) = \mathbb{P}(o_{n+1} \in \{1, 2, \dots, \tau(s_n^{o_n}) - n\}) = \mathbb{P}(o_{n+1} \in \{1, 2, \dots, o_{\max}\}) = 1. \quad (20)$$

Hence, the next augmented state is determined as:

$$\hat{x}_{t+1} = (s_{n+1}^{o_{n+1}}, a_{n+1}, a_{n+2}, \dots, a_t). \quad (21)$$

This implies that if the structure holds at time  $t = n + o_{\max}$ , it continues to hold at the subsequent time step, demonstrating that the structure holds for all  $t = n + o_{\max}$  by induction.

Therefore, the general form of the augmented state is given by:

$$\hat{x}_t = (s_n^{o_n}, a_n, a_{n+1}, \dots, a_{t-1}), \quad \forall t = n + o_{\max}. \quad (22)$$

Substituting  $n = t - o_{\max}$  yields:

$$\hat{x}_t = (s_{t-o_{\max}}^{o_{t-o_{\max}}}, a_{t-o_{\max}}, a_{t-o_{\max}+1}, \dots, a_{t-1}), \quad \forall t > o_{\max}, \quad (23)$$

This formulation is consistent with the structure of the augmented state defined in a CDMDP with constant delay  $\Delta = o_{\max}$ , which can be further reduced to an equivalent delay-free MDP defined over the augmented state space  $(\mathcal{X}, \mathcal{A}, \mathcal{P}_\Delta, \mathcal{R}_\Delta, \gamma)$ . This completes the proof.  $\square$

### D.1 Empirical results for Proposition 4.1

We evaluated the performance of the proposed conservative agent in random-delay environments (conservative-BPQL) against that of the normal agent in constant-delay environments with constant delay  $\Delta = o_{\max}$  (BPQL). The goal was to assess whether both agents exhibit comparable performance, thereby validating the theoretical equivalence. The results are summarized in Table 6 and Fig. 8.

The results demonstrate that both agents achieved *nearly identical* performance across all tasks, providing strong empirical support for our claim that the random-delay environment can be transformed into its constant-delay equivalent through the conservative agent.

Table 6: Results of conservative-BPQL in random-delay environments with delays  $o_{\max} \in \{5, 10, 20\}$  and BPQL in constant-delay environments with delays  $\Delta = o_{\max}$ , evaluated for one million time steps with five different seeds, where the standard deviations of average return are denoted by  $\pm$ .

Environment		Ant-v3	HalfCheetah-v3	Hopper-v3	Walker2d-v3	Humanoid-v3	InvertedPendulum-v2
$o_{\max}$	Algorithm						
5	BPQL (constant)	3761.9 $\pm$ 112	5212.7 $\pm$ 41	2136.3 $\pm$ 158	2577.4 $\pm$ 157	3194.9 $\pm$ 374	955.9 $\pm$ 28
	Conservative-BPQL (random)	3679.8 $\pm$ 167	5583.9 $\pm$ 169	2174.1 $\pm$ 155	2843.2 $\pm$ 272	3157.7 $\pm$ 292	958.8 $\pm$ 14
10	BPQL (constant)	2831.9 $\pm$ 103	4282.2 $\pm$ 203	2129.2 $\pm$ 184	2331.6 $\pm$ 252	2891.5 $\pm$ 357	934.7 $\pm$ 20
	Conservative-BPQL (random)	2744.5 $\pm$ 112	4810.1 $\pm$ 233	2300.9 $\pm$ 164	2122.3 $\pm$ 292	2820.5 $\pm$ 348	936.9 $\pm$ 38
20	BPQL (constant)	2078.9 $\pm$ 157	3062.7 $\pm$ 252	1526.7 $\pm$ 227	846.7 $\pm$ 443	1197.7 $\pm$ 457	608.7 $\pm$ 210
	Conservative-BPQL (random)	1976.5 $\pm$ 248	3727.2 $\pm$ 279	1346.7 $\pm$ 245	1025.7 $\pm$ 302	1143.8 $\pm$ 371	566.9 $\pm$ 88

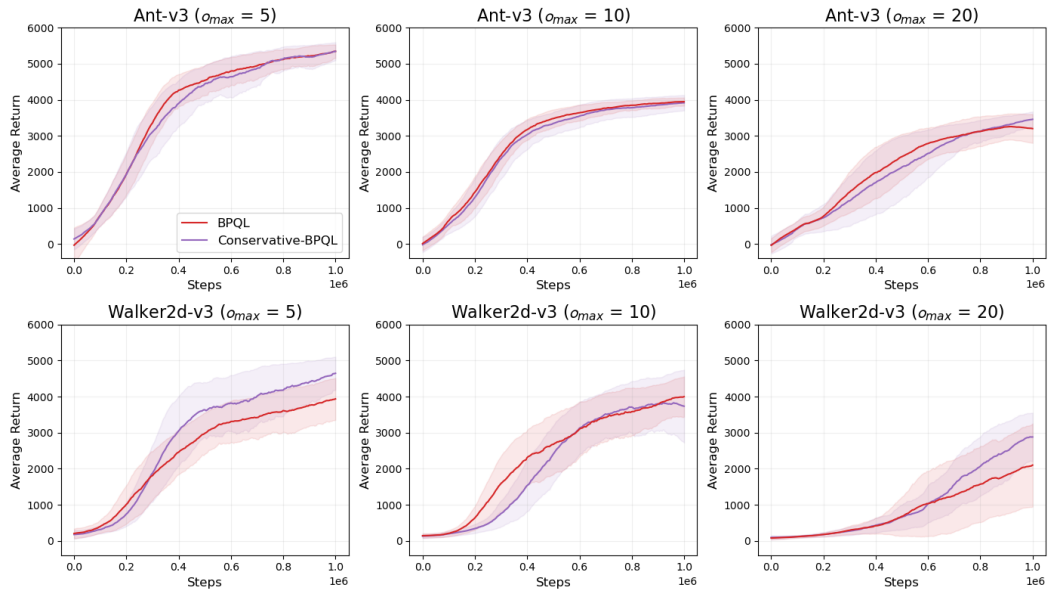


Figure 8: Performance curves of conservative-BPQL agent in random-delay environments with  $o_{\max} \in \{5, 10, 20\}$  and BPQL agent in constant-delay environments with  $\Delta = o_{\max}$  on continuous control tasks in the MuJoCo benchmark. All tasks were conducted with five different seeds for one million time steps, and the shaded regions represent the standard deviation of average returns.

## E Ablation Study

### E.1 Causality in Observations

Under random delays, the observation times of states are scrambled, disrupting the identification of causal relationships between them. Since both complete information methods and model-based approaches rely heavily on understanding these relationships to infer non-delayed information, it becomes challenging for agents to make accurate decisions.

To examine the effect of disrupted causality in observations, we conducted an experiment comparing the performance of agents that make decisions based on the observed order (unordered agent) versus the generated order of states (ordered agent). We employed the delayed-SAC algorithm to train both agents on the InvertedPendulum-v2 task in MuJoCo, as it exhibited the most stable performance in this simple task. Our aim is to investigate how disrupted causality affects the agent’s performance. The corresponding results are presented in Fig. 9.

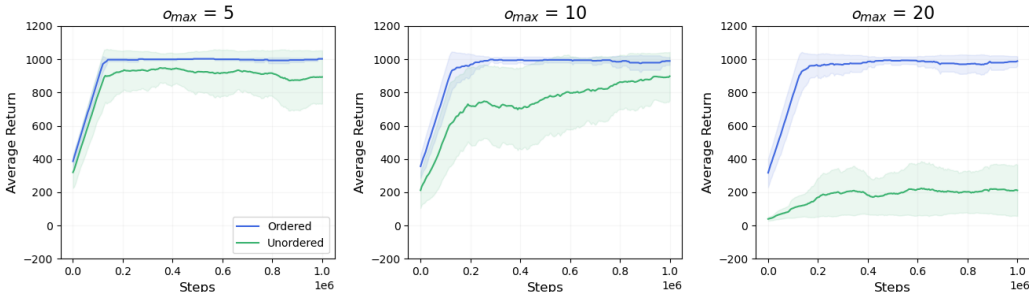


Figure 9: Results of the ordered and unordered agent on the InvertedPendulum-v2 task in MuJoCo under random delays  $o_{max} \in \{5, 10, 20\}$ . Each agent was evaluated for one million time steps with five different seeds, where the shaded regions denote the standard deviation of average returns.

The results reveal that preserving causal consistency in observations significantly affects both the performance and learning stability of RL agents, with performance degradation becoming more pronounced as the randomness of delays increases. Notably, the proposed conservative agent is systematically unaffected by this issue, as it consistently uses temporally appropriate states in their generated order.

## F Experiments Compute Resources

From an implementation perspective, the conservative agent differs from a normal agent only in that it stores observed states in a buffer and processes them in chronological order. This can be efficiently achieved using a priority queue, which supports operations with  $O(\log N)$  time complexity. The computational overhead introduced by the conservative agent arises solely from these operations. Notably, since the number of elements in the queue is at most  $o_{\max}$ , we consider the added overhead to be negligible in practice.

To quantify the computational overhead introduced by the conservative agent, we measured the runtime of BPQL with  $\Delta = o_{\max}$ , conservative-BPQL, and all other baseline algorithms over one million time steps. All experiments were conducted on an NVIDIA RTX 3060 Ti GPU and an Intel i7-12700KF CPU. The results are summarized in Fig. 10. Empirically, the two algorithms—BPQL and conservative-BPQL—exhibit no significant differences in runtime overhead.

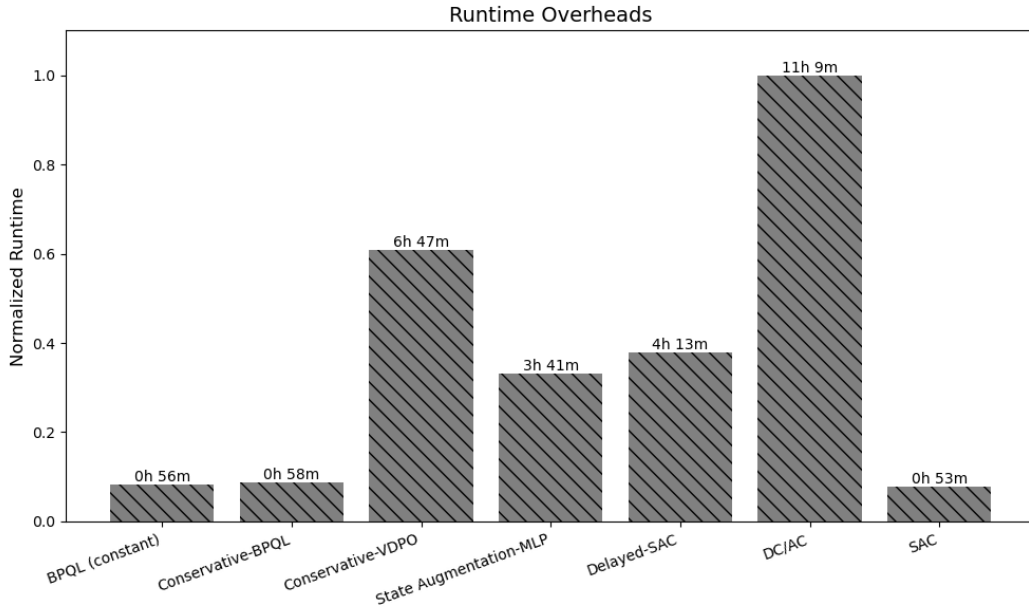


Figure 10: Runtime overheads of each algorithm measured over one million global time steps, tested on an NVIDIA RTX 3060 Ti GPU and an Intel i7-12700KF CPU

## G Limitations

The conservative agent may experience learning inefficiencies under long-tailed delay distributions, as it does not utilize state information available at intermediate time steps. To mitigate this issue, a quantile-based cutoff strategy can be employed.

Specifically, if the delay follows a known long-tailed distribution such as a log-normal distribution, a pseudo maximum allowable delay  $o_{p,max}$  can be defined at a reasonable upper quantile point, such that  $o_{p,max} \ll o_{max}$ . If a state is not observed by this threshold, the agent may instead reuse the most recently used state, assuming the underlying MDP exhibits sufficient smoothness.

We argue that the potential performance degradation from this heuristic is acceptable relative to the significant sample inefficiency incurred by a large  $o_{max}$ . Nonetheless, this strategy assumes prior knowledge of the delay distribution, which may be impractical in certain environments. Addressing this limitation remains an important direction for future research.

## H Visual Representation of Conservative Agent

In this section, we provide a visual representation of the conservative agent-based decision-making process under random delays, where the maximum allowable delay is set to  $o_{\max} = 3$ .

Times	t = 1	t = 2	t = 3	t = 4	t = 5	t = 6	t = 7	t = 8	t = 9	t = 10
Generated states										
Observed states										
Usable states										
Augmented states										
Actions										

(a) Time  $t = 0$

Times	t = 1	t = 2	t = 3	t = 4	t = 5	t = 6	t = 7	t = 8	t = 9	t = 10
Generated states	$s_1^2$									
Observed states										
Usable states										
Augmented states	'no-ops'									
Actions	$a_1$									

(b) Time  $t = 1$

Times	t = 1	t = 2	t = 3	t = 4	t = 5	t = 6	t = 7	t = 8	t = 9	t = 10
Generated states	$s_1^2$	$s_2^1$								
Observed states										
Usable states										
Augmented states		'no-ops'								
Actions	$a_1$	$a_2$								

(c) Time  $t = 2$

Figure 11: At times 1 and 2, the states  $s_1^2$  and  $s_2^1$  are generated but remain unobserved by the agent. In this scenario, the agent does nothing ('no-ops') until the initial state  $s_1^2$  becomes usable.

Times	t = 1	t = 2	t = 3	t = 4	t = 5	t = 6	t = 7	t = 8	t = 9	t = 10
Generated states	$s_1^2$	$s_2^1$	$s_3^2$							
Observed states			$s_1^2$ $s_2^1$							
Usable states										
Augmented states		'no-ops'								
Actions	$a_1$	$a_2$	$a_3$							

(a) Time  $t = 3$ 

Times	t = 1	t = 2	t = 3	t = 4	t = 5	t = 6	t = 7	t = 8	t = 9	t = 10
Generated states	$s_1^2$	$s_2^1$	$s_3^2$	$s_4^3$						
Observed states			$s_1^2$ $s_2^1$							
Usable states				$s_1^2$						
Augmented states		'no-ops'			$\hat{x}_4$					
Actions	$a_1$	$a_2$	$a_3$	$a_4$						

(b) Time  $t = 4$ 

Times	t = 1	t = 2	t = 3	t = 4	t = 5	t = 6	t = 7	t = 8	t = 9	t = 10
Generated states	$s_1^2$	$s_2^1$	$s_3^2$	$s_4^3$	$s_5^1$					
Observed states			$s_1^2$ $s_2^1$		$s_3^2$					
Usable states				$s_1^2$	$s_2^1$					
Augmented states		'no-ops'			$\hat{x}_4$	$\hat{x}_5$				
Actions	$a_1$	$a_2$	$a_3$	$a_4$	$a_5$					

(c) Time  $t = 5$ 

Figure 12: At time 3, states  $s_1^2$  and  $s_2^1$  are observed simultaneously. As the agent uses these observed states at their maximum allowable delayed time steps,  $s_1^2$  is used at time 4 and  $s_2^1$  is used at time 5. These states are reformulated as augmented states before being fed into the policy, thereafter determining the appropriate actions. States  $s_3^2$ ,  $s_4^3$ , and  $s_5^1$  are generated at corresponding times, with  $s_3^2$  being observed at time 5.

Times	t = 1	t = 2	t = 3	t = 4	t = 5	t = 6	t = 7	t = 8	t = 9	t = 10
Generated states	$s_1^2$	$s_2^1$	$s_3^2$	$s_4^3$	$s_5^1$	$s_6^0$				
Observed states			$s_1^2$ $s_2^1$		$s_3^2$	$s_5^1$ $s_6^0$				
Usable states				$s_1^2$	$s_2^1$	$s_3^2$				
Augmented states	'no-ops'			$\hat{x}_4$	$\hat{x}_5$	$\hat{x}_6$				
Actions	$a_1$	$a_2$	$a_3$	$a_4$	$a_5$	$a_6$				

(a) Time  $t = 6$ 

Times	t = 1	t = 2	t = 3	t = 4	t = 5	t = 6	t = 7	t = 8	t = 9	t = 10
Generated states	$s_1^2$	$s_2^1$	$s_3^2$	$s_4^3$	$s_5^1$	$s_6^0$	$s_7^3$			
Observed states			$s_1^2$ $s_2^1$		$s_3^2$	$s_5^1$ $s_6^0$	$s_4^3$			
Usable states				$s_1^2$	$s_2^1$	$s_3^2$	$s_4^3$			
Augmented states	'no-ops'			$\hat{x}_4$	$\hat{x}_5$	$\hat{x}_6$	$\hat{x}_7$			
Actions	$a_1$	$a_2$	$a_3$	$a_4$	$a_5$	$a_6$	$a_7$			

(b) Time  $t = 7$ 

Times	t = 1	t = 2	t = 3	t = 4	t = 5	t = 6	t = 7	t = 8	t = 9	t = 10
Generated states	$s_1^2$	$s_2^1$	$s_3^2$	$s_4^3$	$s_5^1$	$s_6^0$	$s_7^3$			
Observed states			$s_1^2$ $s_2^1$		$s_3^2$	$s_5^1$ $s_6^0$	$s_4^3$			
Usable states				$s_1^2$	$s_2^1$	$s_3^2$	$s_4^3$	$s_5^1$		
Augmented states	'no-ops'			$\hat{x}_4$	$\hat{x}_5$	$\hat{x}_6$	$\hat{x}_7$	$\hat{x}_8$		
Actions	$a_1$	$a_2$	$a_3$	$a_4$	$a_5$	$a_6$	$a_7$	$a_8$		

(c) Time  $t = 8$ 

Figure 13: States  $s_6^0$  and  $s_7^3$  are generated at respective times. At time 6, states  $s_5^1$  and  $s_6^0$  are observed simultaneously but are not immediately usable because the previously generated states,  $s_3^2$  and  $s_4^3$ , have not yet been used in decision-making processes. Instead,  $s_3^2$  is used at this time. At time 7, state  $s_4^3$  is observed and is available for use immediately. At time 8, state  $s_5^1$  becomes usable, as all previously generated states have now been both observed and used.

Times	t = 1	t = 2	t = 3	t = 4	t = 5	t = 6	t = 7	t = 8	t = 9	t = 10
Generated states	$s_1^2$	$s_2^1$	$s_3^2$	$s_4^3$	$s_5^1$	$s_6^0$	$s_7^3$			
Observed states			$s_1^2, s_2^1$		$s_3^2$	$s_5^1, s_6^0$	$s_4^3$			
Usable states				$s_1^2$	$s_2^1$	$s_3^2$	$s_4^3$	$s_5^1$	$s_6^0$	
Augmented states		'no-ops'		$\hat{x}_4$	$\hat{x}_5$	$\hat{x}_6$	$\hat{x}_7$	$\hat{x}_8$	$\hat{x}_9$	
Actions	$a_1$	$a_2$	$a_3$	$a_4$	$a_5$	$a_6$	$a_7$	$a_8$	$a_9$	

(a) Time  $t = 9$ 

Times	t = 1	t = 2	t = 3	t = 4	t = 5	t = 6	t = 7	t = 8	t = 9	t = 10
Generated states	$s_1^2$	$s_2^1$	$s_3^2$	$s_4^3$	$s_5^1$	$s_6^0$	$s_7^3$			
Observed states			$s_1^2, s_2^1$		$s_3^2$	$s_5^1, s_6^0$	$s_4^3$			$s_7^3$
Usable states				$s_1^2$	$s_2^1$	$s_3^2$	$s_4^3$	$s_5^1$	$s_6^0$	$s_7^3$
Augmented states		'no-ops'		$\hat{x}_4$	$\hat{x}_5$	$\hat{x}_6$	$\hat{x}_7$	$\hat{x}_8$	$\hat{x}_9$	$\hat{x}_{10}$
Actions	$a_1$	$a_2$	$a_3$	$a_4$	$a_5$	$a_6$	$a_7$	$a_8$	$a_9$	$a_{10}$

(b) Time  $t = 10$ 

Times	t = 1	t = 2	t = 3	t = 4	t = 5	t = 6	t = 7	t = 8	t = 9	t = 10
Generated states	$s_1^2$	$s_2^1$	$s_3^2$	$s_4^3$	$s_5^1$	$s_6^0$	$s_7^3$			
Observed states	[Observed states are obscured by a grey bar]									
Usable states				$s_1^2$	$s_2^1$	$s_3^2$	$s_4^3$	$s_5^1$	$s_6^0$	$s_7^3$
Augmented states		'no-ops'		$\hat{x}_4$	$\hat{x}_5$	$\hat{x}_6$	$\hat{x}_7$	$\hat{x}_8$	$\hat{x}_9$	$\hat{x}_{10}$
Actions	$a_1$	$a_2$	$a_3$	$a_4$	$a_5$	$a_6$	$a_7$	$a_8$	$a_9$	$a_{10}$

(c) Time  $t = 10$ 

Figure 14: At times 9 and 10, states  $s_6^0$  and  $s_7^3$  are used in sequence. Despite the state observations occurring simultaneously or being out of order, all the delayed states are consistently used in sequence at their maximum allowable delayed time steps, that is,  $\tau(s_n^{o_n}) = n + o_{\max}, \forall n > 0$ .